

# Protection of subterranean water infrastructure in an abrupt sunlight reduction scenario

Baxter L. M. Williams <sup>a,\*</sup>, Xiaofei Feng <sup>a</sup>, Juan Esteban Lamilla Cuellar <sup>b</sup>, Rorik Peterson <sup>c</sup>,  
David Denkenberger <sup>a,b</sup>

<sup>a</sup> Department of Mechanical Engineering, University of Canterbury  
69 Creyke Road  
Christchurch 8041  
New Zealand

<sup>b</sup> Alliance to Feed the Earth in Disasters (ALLFED)  
Lafayette, CO  
USA

<sup>c</sup> Department of Mechanical Engineering, University of Alaska Fairbanks  
PO Box 755905  
Fairbanks, Alaska 99775-5905  
USA

\* Corresponding author: Baxter L. M. Williams ([baxter.williams@pg.canterbury.ac.nz](mailto:baxter.williams@pg.canterbury.ac.nz))

**This paper is a non peer-reviewed preprint submitted to EarthArXiv.**

# **Protection of subterranean water infrastructure in an abrupt sunlight reduction scenario**

## **Abstract**

An abrupt sunlight reduction scenario (ASRS) could result from a nuclear war, supervolcanic eruption, or asteroid/comet impact, reducing global temperatures for over a decade and leaving subterranean water pipes vulnerable to freezing. This paper builds on previous work assessing the extent of vulnerable water pipes in a severe ASRS, and assesses the feasibility of two methods of pipe protection: (i) piling soil above the pipes, and (ii) installing electrical resistive heat cables around pipes. Total vulnerable pipe length is expected to be 5.4-8.8 million km affecting over 2 billion people, with peak freeze depths exceeding 30 m. In several assessed scenarios, soil piling is expected to take 113-141 days and leave 0.32-0.64 million km of pipelines damaged, affecting 161 million people. Heat cables could be installed where soil piling is impractical, such as where pipes are beneath critical roads, but heat cable production is expected to be sufficient for less than 1% of vulnerable pipes. Implications for local, national, and international response planning are discussed, and potential directions for future research are identified, including improved quantification of the extent of subterranean infrastructure, analysis of direct damage from an ASRS-causing event, and exploration of alternative infrastructure protection methods.

**Keywords:** Existential risk, Global catastrophic risk, Nuclear winter, Arctic engineering, Ground freezing, Water pipes

**Word count:** 5403

# 1. Introduction

A nuclear war, supervolcanic eruption, or large asteroid/comet impact could release immense amounts of aerosol materials, such as sulphates or black carbon, into Earth's stratosphere, where they would remain for several years and block incident sunlight [1]. The probability of such an event, known as an abrupt sunlight reduction scenario (ASRS), is estimated to be on the order of 0.1% to 1% per year [2]. An ASRS would decrease global temperatures and precipitate rapid, widespread climate changes [1], and could cause an unrecoverable collapse of civilisation, affecting countless future generations, so is considered an existential risk to humanity [3].

While prevention of such events is preferable in all cases, preventive efforts are not guaranteed to succeed, so investigation of response and resilience is also required [4]. As such, the impacts of, and resilience to, a severe ASRS have been the subject of previous research. An ASRS would cause regional infrastructure destruction and reduce energy generation from wind and solar sources [5]. Additionally, the impacts of an ASRS on food supply would be acute. Storing sufficient food for the duration of an ASRS is expensive and infeasible if the catastrophe were to occur soon, meaning provision of adequate food following an ASRS would likely depend on rapidly scalable resilient food sources [6]. These resilient foods include those not dependent on sunlight, and those with lower sunlight requirements than traditional foods [7]. Resilient foods have been analysed based on their present costs [8], and further research has investigated protein extraction from leaves [9], transforming cellulose into sugar [10], production of natural gas- [11] and hydrogen- [12] consuming single-cell protein (SCP), greenhouses to increase food production [13], seaweed [14], and the nutrition of resilient foods [15,16].

While the effects of an ASRS on food and energy supplies have been the subject of a growing

body of research, the direct impacts of reduced temperatures on infrastructure are less well-studied. Temperature reductions can affect above-ground infrastructure by weakening material or causing contractions. For example, reduced temperatures can cause embrittlement of welds in metal rails, leading to cracks which reduce weld strength [17,18]. Additionally, reduced temperatures can cause the rails themselves to contract, increasing mechanical stress on joints and increasing the probability of breaking under load. While these effects are well understood, their increased frequency and severity following an ASRS would necessitate increased resources for inspections and maintenance.

Temperature reductions could also affect subterranean infrastructure, including pipes carrying fresh water and/or sewage. While soil expansion can cause heaving of these systems and damage critical infrastructure, expansive soils are uncommon [19]. However, the drastically reduced temperatures in an ASRS could freeze the liquid in pipes, causing bursts and extensive damage.

Previous research has assessed the extent of subterranean pipes vulnerable to an ASRS [20], but has not investigated methods to protect this infrastructure to ensure continuity of critical services. A range of interventions could prevent freezing of pipes. If above-ground conditions permitted, insulation could be increased by piling biomass, gravel, or soil. Biomass, such as leaves and sawdust, would provide the best insulation, but would be required for other applications in an ASRS, such as in the food system [21], so would likely be unavailable for infrastructure protection. Of the remaining two, soil is less expensive, less air permeable, and more ubiquitous than gravel, so is expected to be the most likely method of increasing pipe insulation. Where material cannot be piled atop the ground to provide additional insulation, such as when the pipes are located beneath critical roads, other options exist to prevent freezing.

Various potential solutions exist: (i) excavating around pipes and installing electric resistance heating ("heat cable") and insulation, then backfilling the hole; (ii) removing the pavement/concrete to install insulation, then replacing the road surface (however, with no source of heat, the required thickness of insulation is expected to be impractical); (iii) burying the pipes deeper, which would be complicated given the interruption of service; (iv) installing a two-pipe system with water recirculation, which is commonly employed in areas with permafrost [22] but would require service interruption and additional piping costs; (v) deploying an electric heating element within the pipes; and (vi) heating water entering single pipes, which would require increased flow rates and energy costs, and thus may not be generally feasible. Of these options, installing heat cable around vulnerable pipes is expected to be the most viable.

This work builds on previous work assessing the extent of vulnerable subterranean pipes in an ASRS [20], and assesses the two methods considered the most feasible for protecting subterranean pipes in an ASRS: (i) piling additional soil on top of the ground above the pipes; and (ii) adding heat cables and additional insulation to excavated pipes. Data on the extent of vulnerable pipes are obtained from previous work, and heat transfer models are used to determine the effects of different pipe protection methods. The scalability of pipe protection using current resources is calculated, and important considerations for local, national, and international infrastructure protection efforts are discussed.

## **2. Methods**

Global ground temperatures are obtained from the climate model developed by Coupe et al. [23], which provides global climate data for 20 years following an ASRS caused by a large-scale nuclear exchange between NATO and Russia, in which 150 Tg (150 million tonnes) of

soot is injected into the atmosphere. These freezing depth data are used to inform the type and magnitude of intervention required to prevent freezing of subterranean infrastructure.

## 2.1. Pipe infrastructure

The process to identify vulnerable subterranean water infrastructure is the same as that described fully in previous work [R]. Climate data from Coupe et al. [R], which simulate the global climate response to a 150 Tg soot injection from a Russia-NATO nuclear war, are used to compare soil freeze depths under a nuclear winter scenario with current freeze depths. In countries with sub-zero temperatures, water pipeline locations are estimated from satellite images showing nighttime light and artificial impervious surface areas, to estimate areas with subterranean infrastructure. Total vulnerable pipeline lengths are then calculated using two methods, the results of which are validated with case studies in regions with available data, as described in [20]:

**Method 1:** Population data are collected from the LandScan global population raster [24].

Using the relationships described in [25], pipe length is calculated:

$$L_{\text{pipe},i} = 0.01 \text{ Pop}_i^{0.9} \quad (1)$$

where  $L_{\text{pipe},i}$  and  $\text{Pop}_i$  are the pipe length [km] and total population, respectively, of region  $i$ .

**Method 2:** Street network data are collected from OpenStreetMap [R]. Using the relationships described in [26], pipe length is calculated:

$$L_{\text{pipe},i} = 0.641 L_{\text{road},i} \quad (2)$$

where  $L_{\text{road},i}$  is the total road length in region  $i$  [km].

## 2.2. Change in freezing depth

A transient, two-dimensional heat transfer model is constructed in COMSOL Multiphysics (Version 6.1: <https://www.comsol.com/release/6.1>) to quantify the volume of soil required to achieve the same distance between the maximum depth of freeze (F) and the underground pipe as present pre-catastrophe. For example, if F is 0.5 meters above the underground infrastructure pre-catastrophe, the size of soil pile required to ensure F would still be 0.5 meters above the infrastructure in an ASRS is calculated.

The 2-dimensional geometry is shown in Figure 1. This cut plane runs perpendicular to infrastructure such as a pipe, and the right-hand edge of the image is a plane of symmetry. The original ground surface is at the middle dashed line. The amount of soil excavated (“excavated volume”) is equivalent to the trapezoidal region below this line. This excavated volume is thus the same as the trapezoidal region above the middle dashed line on the right (“New volume” with height H; the pile will initially have greater volume but settle to height H).

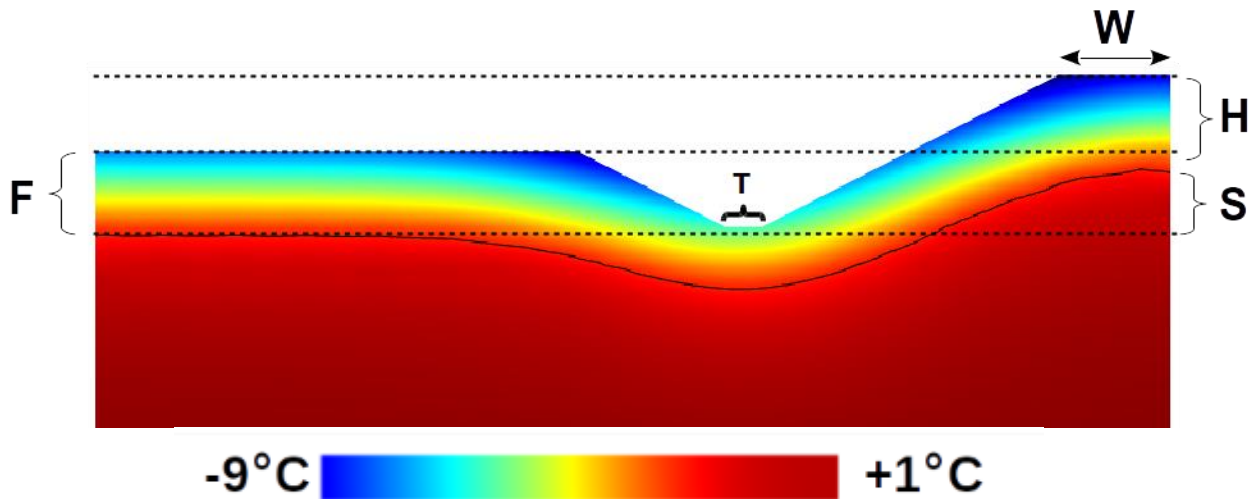


**Figure 1.** Soil piling geometry, showing one half of the symmetrical pile above a pipe (perpendicular to pipe axis, with pipe center at image’s right-hand edge, which is a plane of symmetry).  $H$  is the height of the soil pile,  $W$  is the half-width of the soil pile,  $T$  is the width of the trough for sourcing soil, and  $S$  is the elevation of the freeze depth caused by the pile. Temperature scale is shown for reference, for a  $-10^{\circ}\text{C}$  ambient temperature.

The following assumptions are made about the geometry of the excavation and the pile, and physical properties of the soil:

1. Equal amounts of soil are excavated from both sides to minimize the depth of the excavated volume. In reality, the shape may depart from Figure 1 given constraints of soil availability, such as in cities, and utility of other infrastructure, such as roads.
2. The pile is of a symmetric, trapezoidal shape with half-width of dimension  $W$  on the top.
3. The volume of soil excavated is the same as the volume of soil added.
4. The angle of repose of the pile corresponds to a 50% grade (2-to-1 ratio) of  $26.56^{\circ}$  from horizontal, as this angle is likely the maximum stable slope for unreinforced soil [27,28].
5. Average physical properties of the soil are:  $2000\text{ kg/m}^3$ ,  $800\text{ J/kg}\cdot\text{K}$ ,  $1\text{ W/m}\cdot^{\circ}\text{C}$ , 30% porosity by volume, and 50% saturation of the pores with water (by volume).

Assumptions 1-4 yield the geometric constraint  $W = H + T$ . That is, the half-width of the soil pile ( $W$ ) is equal to the sum of the pile height ( $H$ ) and trough width ( $T$ ). The trough width  $T$  is set at 0.1 meters, recognizing this dimension will ideally be minimized but difficult to obtain zero. With these assumptions and constraints, the only unconstrained geometric parameter is

soil pile height  $H$ , which is defined through a transient freezing simulation.

The freezing front (the  $0\text{ }^{\circ}\text{C}$  isotherm at the interface between frozen and unfrozen soil) progresses downward as temperatures decrease following an ASRS. The depth of frozen material at any time differs along the lateral width shown in Figure 1, due to the varying topography. At a suitable distance (the left side of Figure 1), the effects of the excavation and soil pile are negligible, yielding a one-dimensional (top-down only) freezing process. Thus, the freezing depth  $F$  (distance between the bottom two horizontal lines in Figure 1) represents the undisturbed freezing depth. If the original freezing front location is traced across the figure to the right, the dimension  $S$  represents how far the freezing front is displaced upward from its location without the soil pile. Thus,  $S$  represents the distance of “freeze protection”: the vertical displacement of the freezing front caused by the soil pile. In summary, a soil pile of height  $H$  results in the depth of freeze being moved upward a distance  $S$  from the depth  $F$  it would be without the soil pile.

### **2.3. Earthmoving capacity**

Excavator machinery is classified as belonging to one of four categories to determine earthmoving capacity: small, medium, medium-large, and large [29]. Machines in each category are assumed to be equipped with the smallest bucket commonly used on machines of that size, as smaller buckets are more useful for excavating frozen ground because of the higher pressure they can exert while digging.

In addition to excavator size, earthmoving capacity is affected by the following factors:

- **Frost depth:** Increasing frost depth reduces the bucket filling factor, as frozen soil requires more force to break and can be packed less tightly than unfrozen soil.

- **Cycle time:** Cycle time represents the duration of one complete excavation cycle. Smaller machines typically have faster cycle times.
- **Operator skill, machine availability, and job efficiency:** Total earthmoving capacity increases with increasing operator skill, machine availability, and job efficiency.
- **Bucket capacity:** Larger buckets can move more soil per cycle but distribute excavator force over a greater area, so may be less effective at digging frozen ground.

As operator skill, machine availability, and job efficiency all affect earthmoving capacity [29], the number of effective cycles per hour  $\varepsilon$  [hour<sup>-1</sup>] is assumed to be:

$$\varepsilon = k_{\text{skill}} k_{\text{availability}} k_{\text{efficiency}} (60 / t_{\text{cycle}}) \quad (3)$$

where  $t_{\text{cycle}}$  is the cycle time [minutes], and  $k_{\text{skill}}$ ,  $k_{\text{availability}}$ , and  $k_{\text{efficiency}}$  are unitless coefficients for operator skill, machine availability, and job efficiency, respectively. In these analyses, the coefficients are assumed to be  $k_{\text{skill}} = 0.75$ ,  $k_{\text{availability}} = 0.85$ , and  $k_{\text{efficiency}} = 0.83$ , based on typical values from industry handbooks [29].

The total earthmoving capacity of a machine,  $C_{\text{earthmoving}}$  [m<sup>3</sup>/hour], is calculated according to the cycles per hour and bucket capacity  $C_{\text{bucket}}$  [m<sup>3</sup>]:

$$C_{\text{earthmoving}} = \varepsilon C_{\text{bucket}} \quad (4)$$

Earthmoving productivity per machine, for machines of different sizes, is shown in Table 1.

**Table 1.** Earthmoving productivity for different machine sizes in varying frost depth conditions.

Machine size	Frost depth [m]	$t_{\text{cycle}}$	$\epsilon$ [hour <sup>-1</sup> ]	$C_{\text{bucket}}$ [m <sup>3</sup> ]	$C_{\text{earthmoving}}$ [m <sup>3</sup> /hour]
Small	0 - 0.5	0.26	120	0.21	26
	0.5 - 1	0.28	110	0.20	22
	1+	0.32	100	0.18	19
Medium	0 - 0.5	0.32	100	0.81	82
	0.5 - 1	0.36	89	0.77	68
	1+	0.39	81	0.72	59
Medium-Large	0 - 0.5	0.42	77	1.4	100
	0.5 - 1	0.53	60	1.3	76
	1+	0.57	56	1.2	68
Large	0 - 0.5	0.40	80	1.8	140
	0.5 - 1	0.51	63	1.7	110
	1+	0.63	50	1.6	81

Four scenarios for soil piling are modeled, with the following criteria for distributing excavators: (1) prioritizing pipes with the largest earthmoving requirements; (2) prioritizing areas of immediate concern (i.e., pipes which would freeze first, dynamically relocating excavators to location where freezing is next to occur); (3) evenly distributed by area; and (4) distribution by impacted pipeline length. A total of 2 million excavators are assumed to be available for pipe protection [30], with an average earthmoving capacity of  $C_{\text{earthmoving}} = 19$  m<sup>3</sup>/hour (conservatively assuming the minimum earthmoving rate). A delay of one month is assumed in all scenarios, to allow time for assessment of the catastrophe, planning, and the distribution of equipment, as in similar analyses [30]. To estimate the benefits of the protection measures under various scenarios, population impacts are assessed by overlaying the predicted pipe locations and freezing zones with the LandScan population raster [24]. Population counts are then summed by the model based on whether the underlying pipelines freeze before the protection measures can be implemented.

## 2.4. Heat cable analysis

Where protecting infrastructure with soil would require infeasible pile heights or affect other

uses, such as where pipes are beneath critical roads, heat cables can be installed to actively heat pipes with resistive heating. The rate of heat transfer  $\dot{Q}$  [W/m] from an uninsulated subterranean pipe to the ground surface is calculated:

$$\dot{Q}_{\text{pipe, uninsulated}} = f_{\text{shape}} k_{\text{soil}} (T_{\text{surf}} - T_{\text{pipe}}) \quad (5)$$

where  $k_{\text{soil}}$  is the thermal conductivity of the soil [ $\text{Wm}^{-1}\text{K}^{-1}$ ],  $T_{\text{surf}}$  is the ground surface temperature [K], in these calculations assumed to be the average in a severe ASRS of approximately  $-10\text{ }^{\circ}\text{C}$  [23],  $T_{\text{pipe}}$  is the pipe temperature [K], assumed to be a minimum of  $5\text{ }^{\circ}\text{C}$  to avoid freezing, and  $f_{\text{shape}}$  is the shape factor [dimensionless], defined:

$$f_{\text{shape}} = 2 \pi / \ln(4 z / D) \quad (6)$$

where  $z$  is the burial depth [m], and  $D$  is the pipe diameter [m]. This formulation assumes the pipe is sufficiently long to treat the heat transfer as a two-dimensional problem in the radial and vertical directions [31].

With additional insulation between the heat cable and soil, the rate of heat transfer from the pipe to the ground surface becomes:

$$\dot{Q}_{\text{pipe, insulated}} = U A (T_{\text{surf}} - T_{\text{pipe}}) \quad (7)$$

where  $A$  is the surface area of the pipe [ $\text{m}^2$ ], and  $U$  is the overall heat transfer coefficient between the pipe and ground [ $\text{Wm}^{-2}\text{K}^{-1}$ ]:

$$U = [(r_1/k_{\text{ins}})\ln(r_e/r_1) + (r_1/k_{\text{soil}})\ln(2z/r_e)]^{-1} \quad (8)$$

where  $r_1$  is the pipe radius [m],  $k_{\text{ins}}$  is the thermal conductivity of the insulation [ $\text{Wm}^{-1}\text{K}^{-1}$ ], and  $r_e$  is the outside radius of insulation [m].

Where a unit length of heat cable is insufficient to heat a unit length of pipe, heat cable can be wrapped around the pipe to increase the total heat provided, such as by wrapping the pipe on an angle, rather than applying the heat cable in a straight line along one side of the pipe. For a pipe with known heat loss and a heat cable which can provide heat of  $P_{\text{cable}}$  per unit length of cable [W], the wrap factor  $f_{\text{wrap}}$ , denoting the length of heat cable required per unit length of pipe, is calculated:

$$f_{\text{wrap}} = (\dot{Q}_{\text{pipe}} / L) / P_{\text{cable}} \quad (9)$$

With the wrap factor calculated for an insulated or uninsulated pipe, the length of heat cable required to prevent pipe freezing is calculated. Input parameters for heat cable analysis are shown in Table 2. Insulation is assumed to be provided by extruded polystyrene (XPS) foam, due to its ubiquity, high thermal insulation, and ability to withstand the pressure caused by soil above it.

**Table 2.** Input parameters for analysis of representative heat cable.

Parameter	Value	Source
Diameter of pipe $D$	0.2 m	
Distance from ground to pipe $Z$	1 m	
Shape factor $f_{\text{shape}}$	2.1	
Temperature difference $\Delta T$	15 °C	[1]
Required electrical power per meter	9.84 W	[32]
Heat cable cost per meter	23.4 USD	[32]
Maximum cable circuit length	219 m	[32]
XPS foam price (average per square meter)	4.23 USD / cm	[33,34]

### 3. Results

Peak freezing depths in the ASRS are shown in Figure 2, with 86 countries expected to experience freezing of subterranean infrastructure without intervention. Note the model only calculates depths up to 35 m, and high latitude areas experiencing no increase in freezing depth are already under permafrost. Total global length of vulnerable subterranean pipelines is

calculated to be 5.4 million km using Method 1, and 8.8 million km using Method 2. To provide conservative results and reflect the better performance of Method 2 in validation case studies [20], the total global length of vulnerable pipes is assumed to be 8.8 million km.

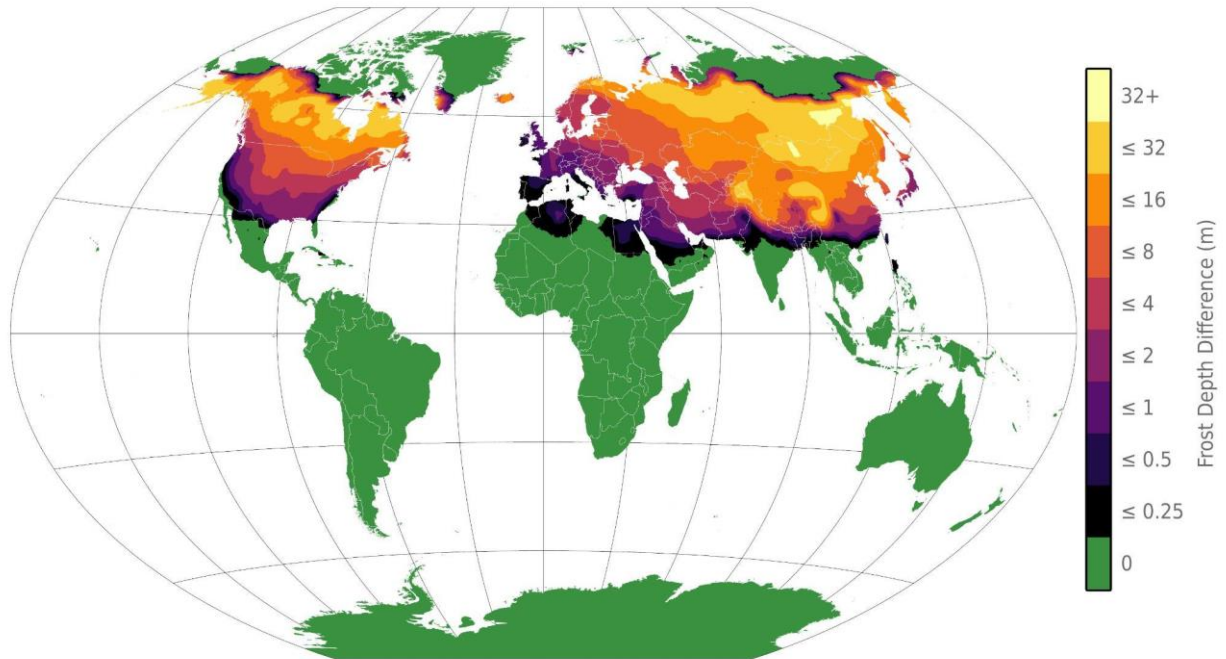


**Figure 2.** Map showing peak difference in freezing depth, which occurs 3 years after the onset of ASRS.

### 3.1. Soil piling

Required soil height (H) for combinations of freeze protection and change in freeze depth F are shown in Figure 3. For example, if F increases from 2 to 5 meters, a freeze protection of  $S = 5 - 2 = 3$  meters is required. The required soil pile height H for such a scenario (~3.4 m) is thus shown at the location (F=5, S=2).

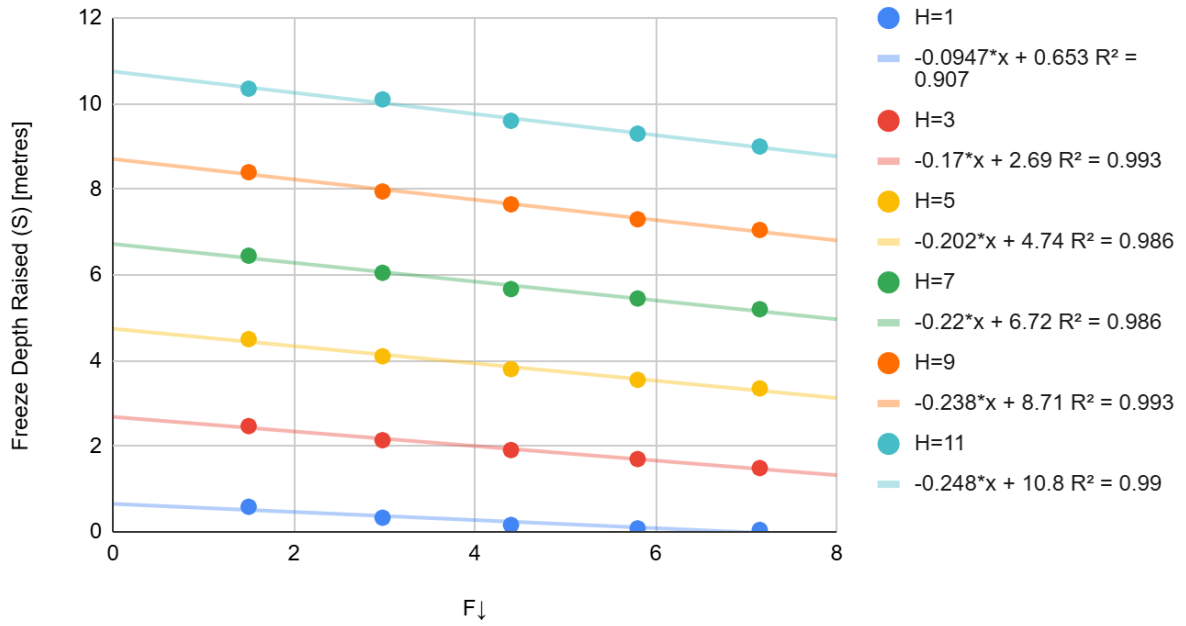


**Figure 3.** Soil pile height (H) required for combinations of freeze depth (F) and freeze protection (S).

The required pile height H, averaged over their at-risk pipe lengths, for countries with the largest requirements are shown in Figure 4. The highest average pile heights are in Mongolia, North Korea, and Kazakhstan, with required pile heights of 14.0, 5.2, and 5.1 meters, respectively. The required average pile height in all but six countries is below four meters.

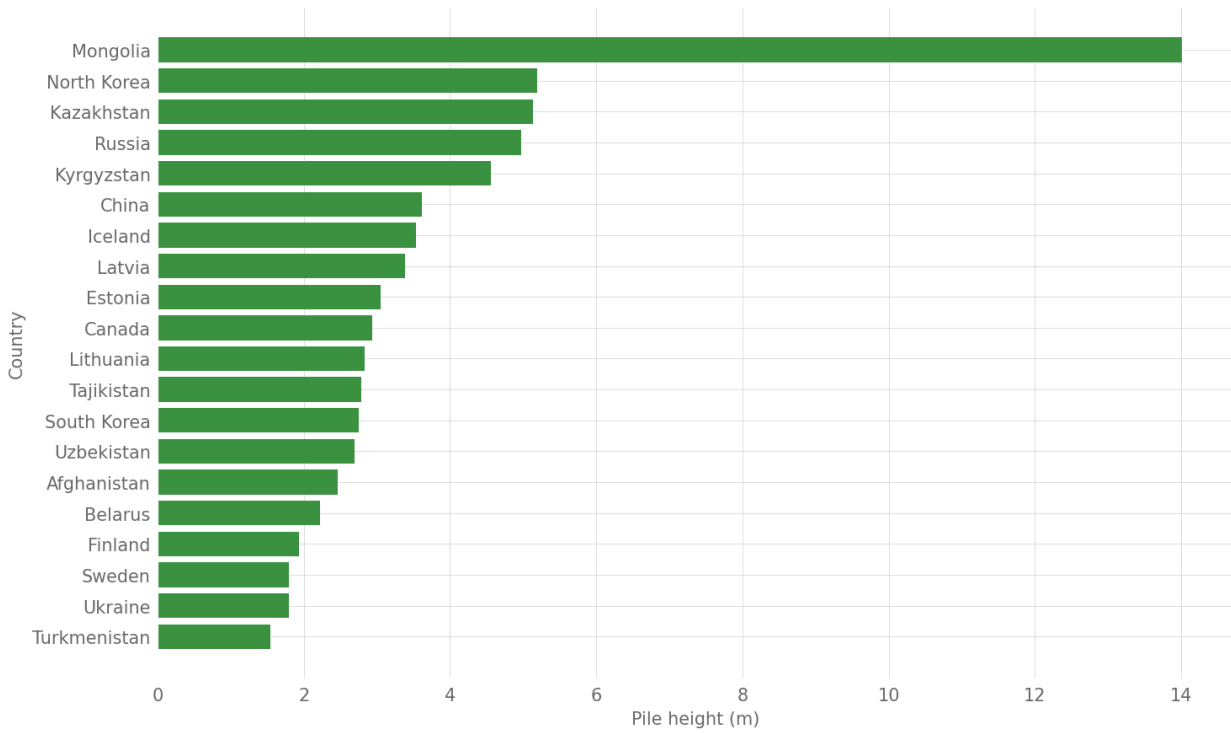


**Figure 4.** Average required pile height (H) for the 20 countries with the largest earthmoving requirements.

### 3.2. Heat cable

Without insulation, a heat cable wrap factor  $f_{wrap}$  of 2.9 is required to maintain pipe temperature above freezing, with a heat loss rate  $\dot{Q}_{pipe,uninsulated}$  of 28.6 W per meter of pipe. The addition of insulation reduces heat loss and required wrap factor, as shown in Table 3.

**Table 3.** Impact of insulation thickness on heat loss and required heat cable length, per meter of pipe, for three insulation thicknesses. Note soil thermal resistance decreases with increasing insulation thickness, to account for the soil displaced by insulation.

	<b>Insulation 1 cm</b>	<b>Insulation 3 cm</b>	<b>Insulation 8 cm</b>
Insulation outside radius $r_e$ [m]	0.11	0.13	0.18
Thermal resistance of the insulation layer $R_{ins}$ [ $m^2 K W^{-1}$ ]	0.35	0.67	1.67
Thermal resistance of the soil $R_{soil}$ [ $m^2 K W^{-1}$ ]	0.32	0.3	0.27
Overall heat transfer coefficient $U$ [ $W m^{-2} K^{-1}$ ]	1.5	1.0	0.52
Heat loss area $A$ [ $m^2/m$ ]	0.71	0.79	1.11
Heat loss $Q_{pipe}$ [W/m]	16	12	8.6
Cable power per meter [W/m]	9.9	9.9	9.9
Required wrap factor	1.6	1.2	0.9

With a maximum cable circuit length of 219 m and power of 9.8 W/m [32], one circuit of heat cable can produce 2.2 kW of heat. At a mains electricity service capacity of 100 A and 240 V, one house can provide 24 kW of power. With a typical peak electricity load in developed countries of 2-15 kW [35,36], which can be further reduced by managing demand [37,38], 9-22 kW could be provided by a typical house. However, even in relatively low density suburban areas with 0.2 hectare plots, the pipe length required to be protected per house would be under 30 m. Thus, heat cable electricity requirements are expected to be met with existing electricity infrastructure in populated areas, which are the areas in which soil piling is most likely to be impractical. If operated continuously, each heat cable circuit's 2.2 kW power demand would require 52 kWh per day. At an average cost of 0.14 USD / kWh [32], heating each run of heat cable would cost 7.25 USD per day (2600 USD/year).

Heat loss, required wrap factor, and costs per meter for insulated and uninsulated pipes are shown in Figure 5. Total cost increases with decreasing insulation, with a total cost of 101 USD per meter of pipe for the uninsulated scenario.

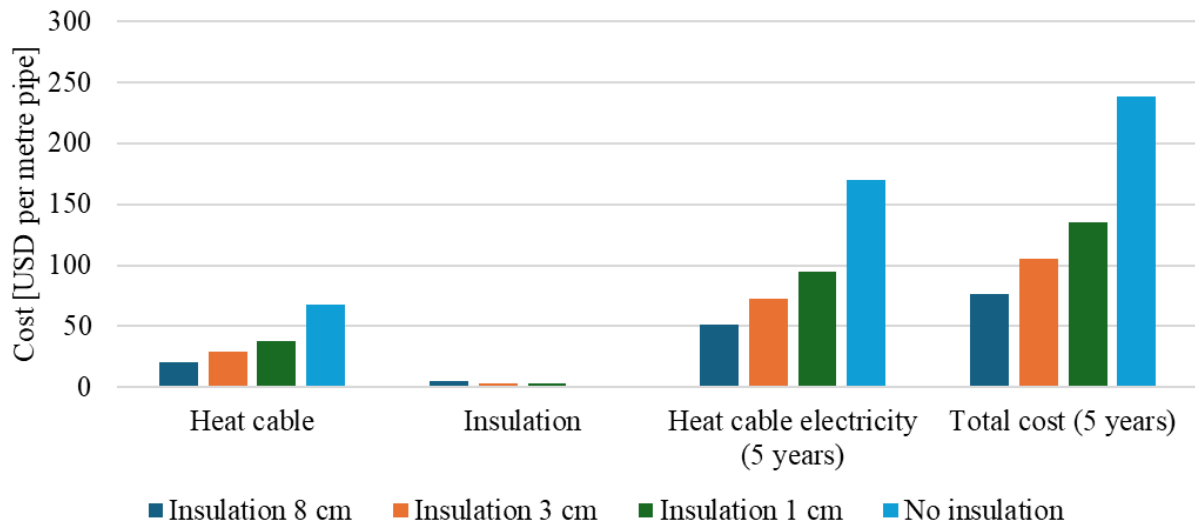


**Figure 5.** Heat cable costs for varying insulation levels.

### 3.3. Scalability

The success of subterranean infrastructure protection in an ASRS will depend on the ability of the proposed solutions to be rapidly deployed before infrastructure is damaged by freezing temperatures. This section provides estimates for the scalability of these solutions.

#### 3.3.1. Earthmoving

Time until maximum protection is achieved varies from 113 to 141 days, as shown in Figure 6. Scenario 2 has the slowest time to achieve maximum required protection but leaves the least damaged pipes, as shown in Table 4. Scenario 2 shows a more variable slope than others, due to the daily relocation of excavators based on predicted freezing depths. This reactive approach helps prevent more pipe damage by quickly addressing emerging risks, but it's also less efficient because resources are constantly being moved. In contrast, the other scenarios focus on completing work in one area before moving on, resulting in smoother trends. Scenario 4 was developed as a compromise—targeting areas with higher pipeline density rather than regions with severe freezing but few pipes, such as parts of Russia and Mongolia.

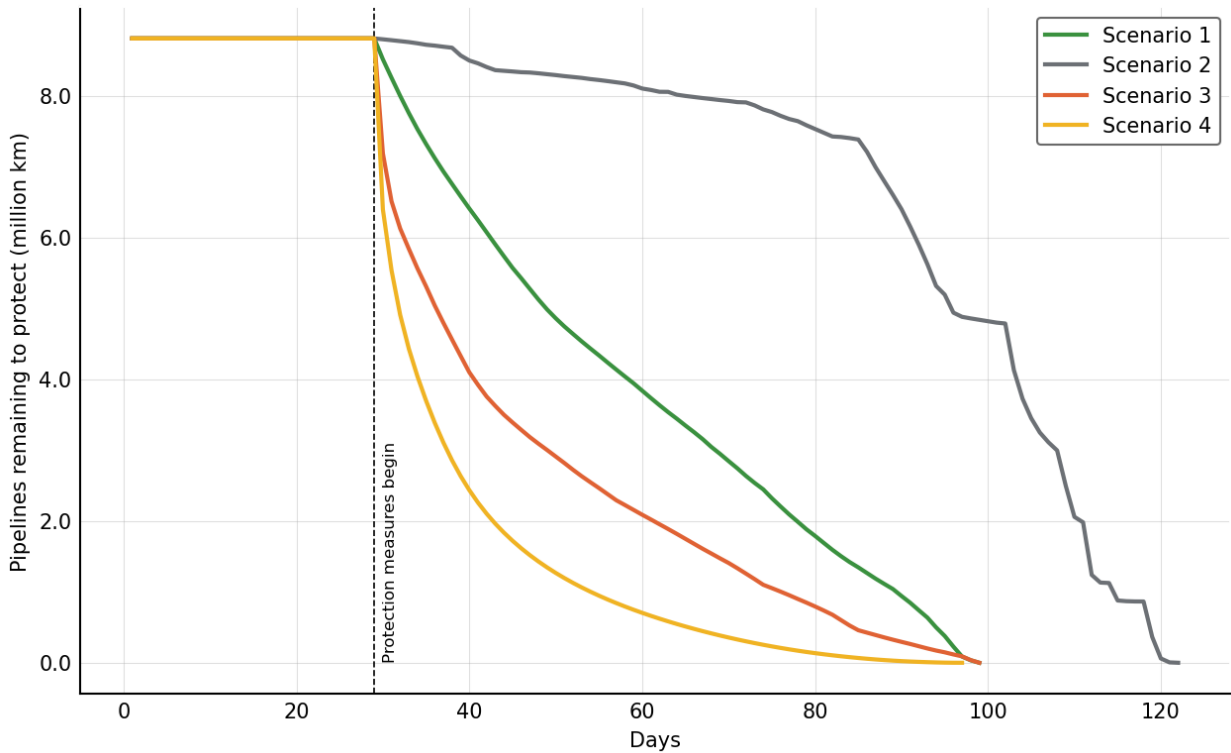


**Figure 6.** Global length of unprotected pipes over time, following onset of ASRS.

### 3.3.2. Impacted population reduction

The estimate for the impacted population without any protection measures stood at approximately 2 billion individuals. As seen in Table 4, with the earthmoving protection measure implemented, this impacted population count could be reduced to 161 million (~92% decrease).

**Table 4.** Time for pipe protection, final length of damaged pipelines, and remaining impacted population for earthmoving Scenarios 1-4.

Scenario	Time until maximum required protection completed [days]	Final damaged pipeline length [km]	Remaining Impacted Population
1	99	0.79 million	314 million
2	122	0.48 million	161 million
3	99	0.76 million	327 million
4	97	0.55 million	230 million

### 3.3.3. Heat cable

The global heat cable market is dominated by cables with metal contacts embedded in a plastic

composite [39] and was valued at 1.5 billion USD in 2023 [40], with 18 major suppliers each producing around 100 km of heat cables per month. Thus, the global heat cable production capacity is approximately 2,000 km per month, or 48,000 km over two years. With wrap factors of 0.9, 1.2, and 2.9 for 8 cm, 3 cm, and 1 cm of insulation, global heat cable production is expected to be sufficient to protect 0.66%, 0.50%, or 0.20%, respectively, of the 8 million km of vulnerable subterranean pipes over the two years before freezing depths reach their maximum depths following an ASRS.

### **3.3.4. Insulation**

With an annual production capacity of 16.8 million tonnes of polystyrene [41] and assuming 10% production losses, annual production capacity of XPS is expected to be 15.1 million tonnes. Polystyrene is expanded during the foaming process to achieve a target density of 35 kg/m<sup>2</sup> [42], yielding a total volume of 430 million m<sup>3</sup>. For an insulation thickness of 8 cm (Table 3), total required area of XPS board is 5.4 billion m<sup>2</sup>. With an average pipeline diameter of 0.2 m and a wrap factor of 1.1, 4.8 billion m<sup>2</sup> of pipe surface area could be covered, for a total distance of 7.8 million km. Thus, insulation production capacity is expected to far exceed heat cable production capacity, so insulation is not expected to be a limiting factor in pipe protection scalability.

## **4. Discussion**

In an extreme ASRS, such as that occurring from a 150 Tg soot injection caused by a nuclear exchange between NATO and Russia, 5.4-8.8 million km of global subterranean water infrastructure is expected to be at risk of freezing. Piling soil on top of at-risk pipes is expected to be sufficient to protect 94% of these pipes. Soil piling is unlikely to be practical for protecting all pipes, as some may require unreasonably large piles or be in locations in which any soil pile

would be impractical. Excavating pipes, installing heat cables, and back-filling soil could prevent water pipes from freezing without compromising above-ground utility. Global heat cable production is expected to be sufficient to protect approximately 0.66% of vulnerable subterranean water pipes over the two years during which freezing depths will be greatest following an ASRS. Thus, heat cables should be reserved for protecting critical pipes unable to be protected by soil piles, such as those beneath critical roads.

In urban and suburban areas, many subterranean water pipes are located beneath roads [43]. Piling soil above these pipes would thus reduce (and, in many cases, completely eliminate) the roads' utility. Thus, trade-offs are expected to arise between transport/accessibility and subterranean infrastructure protection in an ASRS. While heat cables are expected to provide protection for some pipes without compromising accessibility, their limited supply means the vast majority of pipe protection will require soil piling, reducing accessibility. However, in most cities, redundancies exist in both road [44] and water networks [45,46]; i.e., there usually exists more than one route between two locations in a city, both for water and for road vehicles. As such, some roads can be closed, and some water pipes allowed to freeze, without compromising access to transport or water. While trade-offs would be required at the ends of road and water networks, where most houses are served by a single road and water pipe, use of network redundancies is expected to limit utility losses. Plans for subterranean infrastructure protection should thus make full use of these infrastructural redundancies to minimize the amount of unnecessary work and maximize the utility of existing infrastructure.

Global temperatures would decrease rapidly in an ASRS [1], with some pipes expected to freeze within one month of the onset of an ASRS [20]. Thus, the protection of subterranean infrastructure is time-sensitive, as any delays may lead to pipe freezing, which would be far

more resource-intensive to reverse than prevent. As such, governments and local councils should preemptively develop plans to prevent freezing of subterranean infrastructure in an ASRS. Such plans should detail both operational aspects, such as the location of underground pipes and their expected requirements for protection, and procurement, such as of earthmoving equipment and any required heat cables, which are likely to require international cooperation. To increase the likelihood of international cooperation in a catastrophe, governments should also seek to strengthen international ties and to collectively develop international response plans for global catastrophic events, such as an ASRS.

#### **4.1. Limitations and future work**

In this work, soil properties around the world are assumed to be the same. While the thermal and mechanical properties of soil can vary both intra- and inter- regionally [47,48], accounting for these variations would considerably increase both computational and data requirements. As this work aims to provide an overview of the feasibility of different infrastructure protection methods, such variations are outside the scope of this paper. Thus, the results presented in this work should be considered representative of what may be feasible in a severe ASRS, and further research could assess the effects of variation in soil properties on the regional feasibility of these methods.

The total length of subterranean pipes around the world is uncertain, as complete data are unavailable. In this work, pipe lengths in regions vulnerable to freezing in an ASRS are calculated from proxies, such as nighttime light and artificial impervious surfaces to approximate areas likely served by underground pipelines, and correlations between subterranean water pipe lengths and population or above-ground infrastructure. While these estimates and correlations have been validated where reputable data are available, they may

not accurately represent the diversity of water network lengths in at-risk areas. Future work to minimize these uncertainties could conduct field measurements of subterranean water infrastructure and/or investigate more robust correlations with easier-to-measure variables.

Calculations of earthmoving capacity in this work assume the availability of 2 million excavators, with an average capacity of  $C_{\text{earthmoving}} = 19 \text{ m}^3/\text{hour}$ . This average earthmoving capacity is equal to small excavators in the toughest ground conditions, so real capacities may be greater. However, while the total number of excavators is based on previous research on excavator availability in an ASRS [R], this value does not account for competition from other sectors with earthmoving requirements, such as agriculture. Thus, future work could assess the competing needs of various post-catastrophe interventions to determine optimal equipment distributions.

This work models the impacts of an ASRS caused by an injection of 150 Tg soot from a nuclear exchange between NATO and Russia. Direct infrastructure damage is likely to occur during such a nuclear exchange, which could affect the amount of infrastructure requiring protection and the amount of equipment available to protect remaining infrastructure. However, including these effects in this work would require additional assumptions and limit the generalisability of results, especially when comparing the effects of ASRSs caused by other events, such as a supervolcanic eruption or asteroid/comet impact. Thus, the direct effects on infrastructure from the event causing an ASRS (in this case, a nuclear war) are not included in this work. Future work could quantify the impacts of this assumption by comparing scenarios with and without direct infrastructure damage.

These analyses assume international cooperation in infrastructure protection efforts, such as

supply of heat cables and the provision of earthmoving equipment where it is required. In reality, efforts to protect subterranean infrastructure following an ASRS may be hindered by limitations on international cooperation, particularly if the ASRS is caused by an act of international aggression, such as a nuclear war. However, to retain generalisability, the effects of sanctions or other trade restrictions are not included in these analyses. Thus, these results implicitly show the importance of international cooperation in a catastrophe, as limitations on this cooperation could hinder the abilities of all countries to respond to such events.

Future research could investigate the effects of other methods for preventing freezing of subterranean water infrastructure, such as piling snow, installing electric resistance heaters inside vulnerable pipes, and different water heating schemes. The effects of an ASRS on other subterranean infrastructure, such as foundations for buildings, energy networks, and cellphone towers, could also be analyzed. Additionally, future work could assess the potential to rapidly increase heat tape production, such as by repurposing existing factories or investing in small-scale production.

## **5. Conclusions**

A severe abrupt sunlight reduction scenario (ASRS), such as that resulting from a large-scale nuclear exchange between NATO and Russia, is expected to leave 5.4-8.8 million km of global subterranean water pipelines vulnerable to freezing. Piling soils above vulnerable pipes is expected to take between 113-141 days to protect as many pipes as possible, leaving 0.32-0.64 million km damaged, depending on the strategy for pipe prioritization. In areas where soil piling is impractical, heat cables offer a viable alternative for critical pipes, particularly those beneath critical roads, but are expected to be capable of protecting only 0.66% of vulnerable pipes. These results highlight the importance of preemptive planning and international

cooperation to protect subterranean infrastructure in an ASRS. Governments and local councils should develop detailed response plans, including operational aspects and procurement strategies for earthmoving equipment and heat cables. The use of infrastructural redundancies in urban and suburban areas could help to mitigate impacts on transport and water networks. Future research could improve quantification of the extent of subterranean infrastructure, analyze the effects of direct infrastructure damage from the ASRS-causing event, assess the impacts of an ASRS on, and protection methods for, other underground and above ground infrastructure, and investigate alternative methods for preventing pipe freezing.

## Acknowledgements

The authors thank Charles Bardeen and team for global climate data during a nuclear winter, Tim Fist for initiating spatial analysis work, and Alliance to Feed the Earth in Disasters (ALLFED) for funding.

## References

- [1] A. Robock, Nuclear winter, *Wiley Interdiscip Rev Clim Change* 1 (2010) 418–427.
- [2] A.M. Barrett, S.D. Baum, K. Hostetler, Analyzing and Reducing the Risks of Inadvertent Nuclear War Between the United States and Russia, *Science & Global Security* 21 (2013) 106–133. <https://doi.org/10.1080/08929882.2013.798984>.
- [3] T. Maher, S. Baum, Adaptation to and Recovery from Global Catastrophe, *Sustainability* 5 (2013) 1461–1479. <https://doi.org/10.3390/su5041461>.
- [4] O. Cotton-Barratt, M. Daniel, A. Sandberg, Defence in Depth Against Human Extinction: Prevention, Response, Resilience, and Why They All Matter, *Glob Policy* 11 (2020) 271–282. <https://doi.org/10.1111/1758-5899.12786>.
- [5] A.R. Varne, S. Blouin, B.L.M. Williams, D. Denkenberger, The impact of abrupt sunlight reduction scenarios on renewable energy production, *Energies (Basel)* 17 (2024) 5147.
- [6] S.D. Baum, D.C. Denkenberger, J.M. Pearce, A. Robock, R. Winkler, Resilience to global food supply catastrophes, *Environ Syst Decis* 35 (2015) 301–313. <https://doi.org/10.1007/s10669-015-9549-2>.
- [7] S.D. Baum, D.C. Denkenberger, J. Pearce, Alternative foods as a solution to global food supply catastrophes, *Solutions* (2016).
- [8] D. Denkenberger, J. Pearce, A.R. Taylor, R. Black, Food without sun: Price and life-saving potential, *Foresight* 21 (2019) 118–129.

- [9] J.M. Pearce, M. Khaksari, D. Denkenberger, Preliminary Automated Determination of Edibility of Alternative Foods: Non-Targeted Screening for Toxins in Red Maple Leaf Concentrate, *Plants* 8 (2019) 110. <https://doi.org/10.3390/plants8050110>.
- [10] J. Throup, J.B.G. Martínez, B. Bals, J. Cates, J.M. Pearce, D.C. Denkenberger, Rapid repurposing of pulp and paper mills, biorefineries, and breweries for lignocellulosic sugar production in global food catastrophes, *Food and Bioproducts Processing* 131 (2022) 22–39.
- [11] J.B. García Martínez, J.M. Pearce, J. Throup, J. Cates, M. Lackner, D.C. Denkenberger, Methane single cell protein: Potential to secure a global protein supply against catastrophic food shocks, *Front Bioeng Biotechnol* 10 (2022) 906704.
- [12] J.B.G. Martínez, J. Egbejimba, J. Throup, S. Matassa, J.M. Pearce, D.C. Denkenberger, Potential of microbial protein from hydrogen for preventing mass starvation in catastrophic scenarios, *Sustain Prod Consum* 25 (2021) 234–247.
- [13] K.A. Alvarado, A. Mill, J.M. Pearce, A. Vocaet, D. Denkenberger, Scaling of greenhouse crop production in low sunlight scenarios, *Science of the Total Environment* 707 (2020) 136012.
- [14] F.U. Jehn, F.J. Dingal, A. Mill, C. Harrison, E. Ilin, M.Y. Roleda, S.C. James, D. Denkenberger, Seaweed as a resilient food solution after a nuclear war, *Earths Future* 12 (2024) e2023EF003710.
- [15] D. Denkenberger, J.M. Pearce, Micronutrient Availability in Alternative Foods During Agricultural Catastrophes, *Agriculture* 8 (2018) 169. <https://doi.org/10.3390/agriculture8110169>.
- [16] A. Pham, J.B. García Martínez, V. Brynych, R. Stormbjorne, J.M. Pearce, D.C. Denkenberger, Nutrition in abrupt sunlight reduction scenarios: envisioning feasible balanced diets on resilient foods, *Nutrients* 14 (2022) 492.
- [17] Y. Wang, H. Zhou, Y. Shi, B. Feng, Mechanical properties and fracture toughness of rail steels and thermite welds at low temperature, *International Journal of Minerals, Metallurgy, and Materials* 19 (2012) 409–420. <https://doi.org/10.1007/s12613-012-0572-8>.
- [18] L. Ma, L.B. Shi, J. Guo, Q.Y. Liu, W.J. Wang, On the wear and damage characteristics of rail material under low temperature environment condition, *Wear* 394–395 (2018) 149–158. <https://doi.org/10.1016/j.wear.2017.10.011>.
- [19] J.D. Rogers, R. Olshansky, R.B. Rogers, Damage to foundations from expansive soils, *Claims People* 3 (1993) 1–4.
- [20] J.E. Lamilla Cuellar, R. Palm, D. Denkenberger, F. Jehn, Nuclear Winter Could Sever Urban Water Access Across the Northern Hemisphere, (2025). <https://doi.org/10.31223/X5M43H>.
- [21] D. Denkenberger, J.M. Pearce, *Feeding Everyone No Matter What: Managing Food Security After Global Catastrophe*, Academic Press, 2015.
- [22] Y. Pericault, M. Risberg, M. Viklander, A. Hedström, Temperature performance of a heat-traced utilidor for sewer and water pipes in seasonally frozen ground, *Tunnelling and Underground Space Technology* 97 (2020) 103261. <https://doi.org/10.1016/j.tust.2019.103261>.
- [23] J. Coupe, C.G. Bardeen, A. Robock, O.B. Toon, Nuclear winter responses to nuclear war between the United States and Russia in the whole atmosphere community climate model version 4 and the Goddard Institute for Space Studies ModelE, *Journal of Geophysical Research: Atmospheres* 124 (2019) 8522–8543.
- [24] V. Lebakula, J. Epting, J. Moehl, C. Stipek, D. Adams, A. Reith, J. Kaufman, J. Gonzales, B. Reynolds, S. Basford, A. Martin, W. Buck, A. Fazon, A. Cunningham, A. Roy, Z. Barbose, J. Massaro, S. Walters, C. Woody, A. Iman, A. Wilkins, E. Powerll,

- M. Urban, LandScan Silver Edition, Oak Ridge National Laboratory (2023). <https://landscan.ornl.gov/> (accessed April 24, 2025).
- [25] S. Pauliuk, G. Venkatesh, H. Brattebø, D.B. Müller, Exploring urban mines: pipe length and material stocks in urban water and wastewater networks, *Urban Water J* 11 (2014) 274–283. <https://doi.org/10.1080/1573062X.2013.795234>.
- [26] M. Mair, J. Zischg, W. Rauch, R. Sitzenfrei, Where to Find Water Pipes and Sewers?—On the Correlation of Infrastructure Networks in the Urban Environment, *Water (Basel)* 9 (2017) 146. <https://doi.org/10.3390/w9020146>.
- [27] Southern Tier Central Regional Planning & Development Board, Guidance for Determining the Slope, 2021. <https://www.stcplanning.org/wp-content/uploads/2021/07/DeterminingSlope.pdf> (accessed April 24, 2025).
- [28] P. Panagos, P. Borrelli, K. Meusburger, A New European Slope Length and Steepness Factor (LS-Factor) for Modeling Soil Erosion by Water, *Geosciences (Basel)* 5 (2015) 117–126. <https://doi.org/10.3390/geosciences5020117>.
- [29] Caterpillar Inc., Caterpillar Performance Handbook, 49th ed., Peoria, Illinois, 2023. <https://www.warrencat.com/performance-handbook/> (accessed April 24, 2025).
- [30] L. Monteiro, M. Hinge, S. Blouin, M. Rivers, J.D. van der Walt, D. Denkenberger, Expansion of cropland area during an abrupt sunlight reduction scenario, (2024). <https://doi.org/https://doi.org/10.31223/X5MQ54>.
- [31] Y. Çengel, M. Boles, *Thermodynamics: An Engineering Approach*, 10th ed., McGraw-Hill Education, New York, NY, 2023.
- [32] L. Dwyer Instruments, 204 °C Max Constant Wattage Heating Cable 120-480 Vac, (2025). <https://www.dwyeromega.com/en-us/204-c-max-constant-wattage-heating-cable-120-480-vac/p/FE-HEATER> (accessed April 24, 2025).
- [33] The Underfloor Heating Store, XPS Insulation Board, (2025). <https://www.theunderfloorheatingstore.com/products/budget-xps-insulation-boards> (accessed April 24, 2025).
- [34] SteelProfil, XPS Extruded Polystyrene Boards Insulation 80 mm 1250x600mm 8cm, (2025).
- [35] B. Anderson, D. Evers, R. Ford, D. Giraldo Ocampo, R. Peniamina, J. Stephenson, K. Suomalainen, L. Wilcocks, M. Jack, New Zealand GREEN grid household electricity demand study 2014-2018, (2018).
- [36] B. Williams, D. Bishop, G. Hooper, J.G. Chase, Driving change: Electric vehicle charging behavior and peak loading, *Renewable and Sustainable Energy Reviews* 189 (2024) 113953. <https://doi.org/https://doi.org/10.1016/j.rser.2023.113953>.
- [37] B. Williams, D. Bishop, P. Gallardo, J.G. Chase, Demand Side Management in Industrial, Commercial, and Residential Sectors: A Review of Constraints and Considerations, *Energies (Basel)* 16 (2023) 5155.
- [38] B. Williams, D. Bishop, Flexible futures: The potential for electrical energy demand response in New Zealand, *Energy Policy* 195 (2024) 114387. <https://doi.org/10.1016/j.enpol.2024.114387>.
- [39] Heat Trace, Self-Regulating Heating Cables, (2025). <https://www.heat-trace.com/products/self-regulating-heating-cables> (accessed April 24, 2025).
- [40] S.N. Jha, Heating Cable Market Outlook (2023 to 2033), 2025. <https://www.factmr.com/report/730/heating-cable-market> (accessed April 24, 2025).
- [41] Statista, Production capacity of polystyrene worldwide in 2022 and 2026, 2023. <https://www.statista.com/statistics/1065889/global-polystyrene-production-capacity/> (accessed April 24, 2025).
- [42] J.R. Zhao, R. Zheng, J. Tang, H.J. Sun, J. Wang, A mini-review on building insulation materials from perspective of plastic pollution: Current issues and natural fibres as a

- possible solution, *J Hazard Mater* 438 (2022) 129449.  
<https://doi.org/10.1016/j.jhazmat.2022.129449>.
- [43] M.O. Gessner, R. Hinkelmann, G. Nützmann, M. Jekel, G. Singer, J. Lewandowski, T. Nehls, M. Barjenbruch, Urban water interfaces, *J Hydrol (Amst)* 514 (2014) 226–232.  
<https://doi.org/10.1016/j.jhydrol.2014.04.021>.
- [44] A. Sharifi, Resilient urban forms: A review of literature on streets and street networks, *Build Environ* 147 (2019) 171–187. <https://doi.org/10.1016/j.buildenv.2018.09.040>.
- [45] A. Di Nardo, M. Di Natale, C. Giudicianni, D. Musmarra, J.M.R. Varela, G.F. Santonastaso, A. Simone, V. Tzatchkov, Redundancy Features of Water Distribution Systems, *Procedia Eng* 186 (2017) 412–419.  
<https://doi.org/10.1016/j.proeng.2017.03.244>.
- [46] A. Yazdani, P. Jeffrey, Applying Network Theory to Quantify the Redundancy and Structural Robustness of Water Distribution Systems, *J Water Resour Plan Manag* 138 (2012) 153–161. [https://doi.org/10.1061/\(ASCE\)WR.1943-5452.0000159](https://doi.org/10.1061/(ASCE)WR.1943-5452.0000159).
- [47] G.B.M. Heuvelink, R. Webster, Modelling soil variation: past, present, and future, *Geoderma* 100 (2001) 269–301. [https://doi.org/10.1016/S0016-7061\(01\)00025-8](https://doi.org/10.1016/S0016-7061(01)00025-8).
- [48] B.B. Trangmar, R.S. Yost, M.K. Wade, G. Uehara, M. Sudjadi, Spatial Variation of Soil Properties and Rice Yield on Recently Cleared Land, *Soil Science Society of America Journal* 51 (1987) 668–674.  
<https://doi.org/10.2136/sssaj1987.03615995005100030021x>.